Construction of Simulation Model of 'Lushijia No.1' under Wind and Wave Integration

Shuyi Chen [1, *], Yang Li [2]

[1] School of Aeronautic Science and Engineering, Beihang University, HaiDian, Beijing, 100083

[2] Institute of Artificial Intelligence, Beihang University, HaiDian, Beijing, 100083

* Corresponding Author Email: 20374173@buaa.edu.cn

Abstract. Based on the new ' Lu Shijia No.1 ' platform, the project team has customized a set of force and motion response theory system for it. The existing model is extended, and the basic coordinate system of eight frames is proposed for the new platform, which simplifies the analysis process. By considering the design parameters of the platform, the linear potential flow theory, Stokes wave theory and blade element theory are used to analyze the force and motion response of the platform, and the numerical calculation standards of various forces are defined. At the same time, the H ∞ controller of the optimized fan is integrated to improve the overall control system of the fan. Based on the full coupling integration of wind turbine and platform, the project team uses AQWA hydrodynamic analysis software to simulate and analyze the platform in frequency domain. With the help of FAST-matlab, the time domain full coupling analysis of the platform is carried out. The simulation results show that the new ' Lu Shijia No.1 ' achieves the expected effect of ' reducing response and increasing power '. On the basis of simulation, the project team constructed a scaled down ' Lu Shijia No.1 ' model. Through the final launching test of the solid model, the feasibility of the theoretical design was proved.

Keywords: Lu Shijia No.1, Platform optimization design, Platform system dynamics, Simulation, Solid model construction.

1. Introduction

The concept of floating offshore wind power generation was proposed early on by Dr. William E [1-3]. Heronemus, an American, but the technology did not receive renewed attention until the mid-1990s, when wind power technology became heavily commercialized [4-6]. A floating offshore wind turbine (FOWT) is a system of offshore wind power platforms mounted on a floating structure that can be installed in deeper waters. Because the wind is stronger and more stable in the deep ocean environment, making the deep ocean contain a large amount of wind power potential, the economic benefits of floating offshore wind turbines are much higher than those of onshore wind power [7].

2. Simulation of ' Lu Shijia No.1'under random wind and waves

In order to judge the performance of the platform after optimization in many aspects, we adopt ANSYS AQWA software and FAST-matlab joint simulation system for analysis [8-10]. Among them, ANSYS AQWA can analyze from the shape of the model body by dividing micro elements, which is more intuitive and specific in operation and also eliminates the process of adjusting and modifying many parameters; while FAST, as an open source software, is difficult to operate, but its simulation strictly follows the read-in data, and its simulation results are more objective and realistic, and the basic parameters of the wind turbine platform are shown in Figure 1 and Table 1.

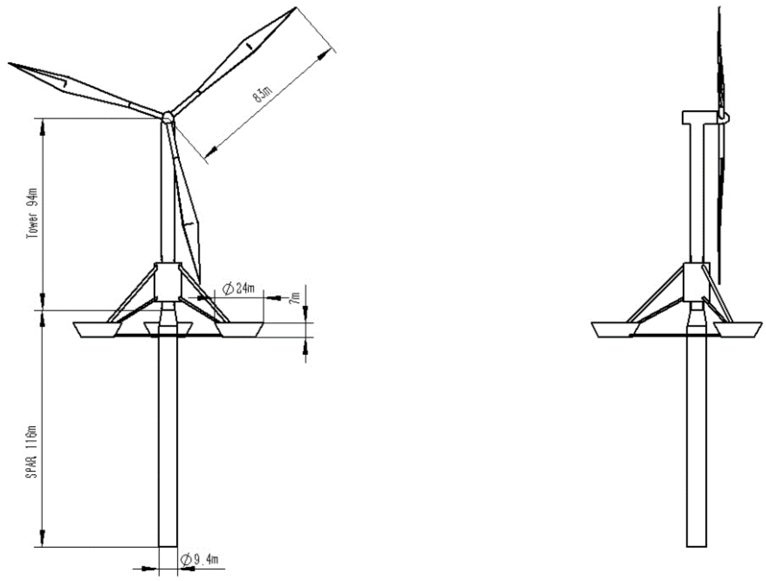

Figure 1. Basic parameters of the platform

Table 1. Parameter design of the Ruzika-1 platform

Indicators	Numerical value
Tower height	94m
Height of column support platform	116m
Effective diameter of column type support platform	9.4m
Blade length	83m
Bushing height	15.59m
Vertical distance between the low end of the bushing and the float	13.83m
Brace a (long) length	38.92m
Spreader bar a (short) length	25.94m
Brace two (horizontal) length	61.11m
Wave energy float height	7m
Wave energy float diameter	24m

2.1. Frequency domain analysis of the motion response of the platform

The frequency domain analysis of the overall wind turbine platform (including the support platform and auxiliary platform) in regular waves can reflect the hydrodynamic performance of the wind turbine platform and design a good platform structure. Since the main period of hydrodynamic response should avoid the main spectral interval of waves in the operating sea as far as possible, the frequency domain analysis can help to select the site for the wind turbine platform and slow down the motion response amplitude of the floating structure in the marine environment, so as to avoid resonance.

2.1.1 JONSWAP wave spectrum

The wave spectrum needs to be introduced in the simulation. Sea spectra such as P-M assume that the sea surface reaches steady state and that the sea spectrum is uniquely related to the wind speed, which is an idealized condition, which is not the case (Figure 2). The most systematic wave observation work to date has yielded the JONSWAP spectrum, which is applied in this paper to describe the non-steady state sea surface with a spectral expression of

$$S(\omega) = \frac{\alpha g^2}{\omega^5} exp\left[-\frac{5}{4}\left(\frac{\omega_0}{\omega}\right)^4\right] \cdot \gamma^{exp\left[-\frac{(\omega-\omega_0)^2}{2\sigma^2\omega_0^2}\right]} \tag{1}$$

where ω_0 is the peak frequency. γ is the peak elevation factor (the observed value is between 1.5~6, the average value is 3.3). σ is the peak shape parameter, the causeless constant $\alpha = 0.076\overline{X}^{-0.22}$; the causeless wind region $\overline{X} = \frac{gX}{U_{10}^2}$ (X is the wind region and $\overline{X} \in (0.1, 10^5)$, U_{10} is the wind speed at a height of 10 meters).

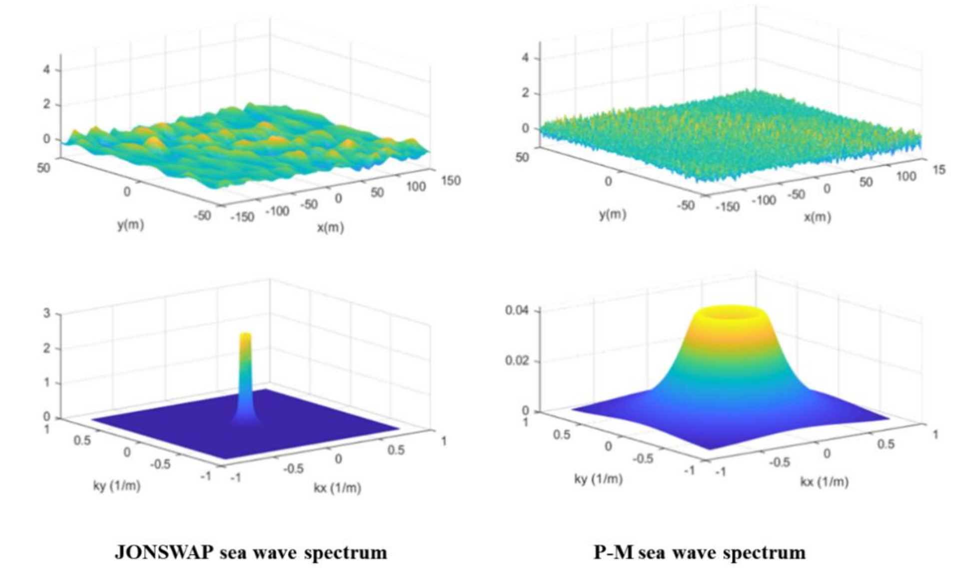

Figure 2. Comparison of spectral shape and wave number spectra of JONSWAP and P-M wave spectrucm

2.1.2 Comparative analysis of platforms under random wave iterations

The JONSWAP wave spectrum introduced above is used as the random wave for the simulation below. Under the same random wave interference, the relationship between the corresponding motion response angle and the change of iteration steps of the two platform systems is obtained through the simulation of AQWA (Figures 3 and 4).

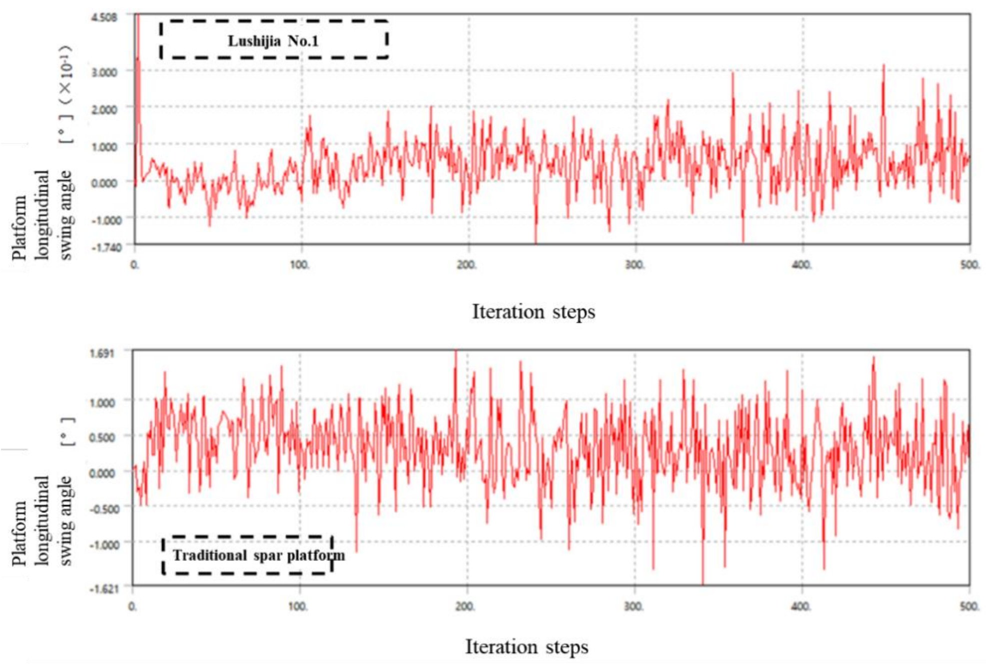

Figure 3. Random response images of the platform under JONSWAP spectrum (vertical shake)

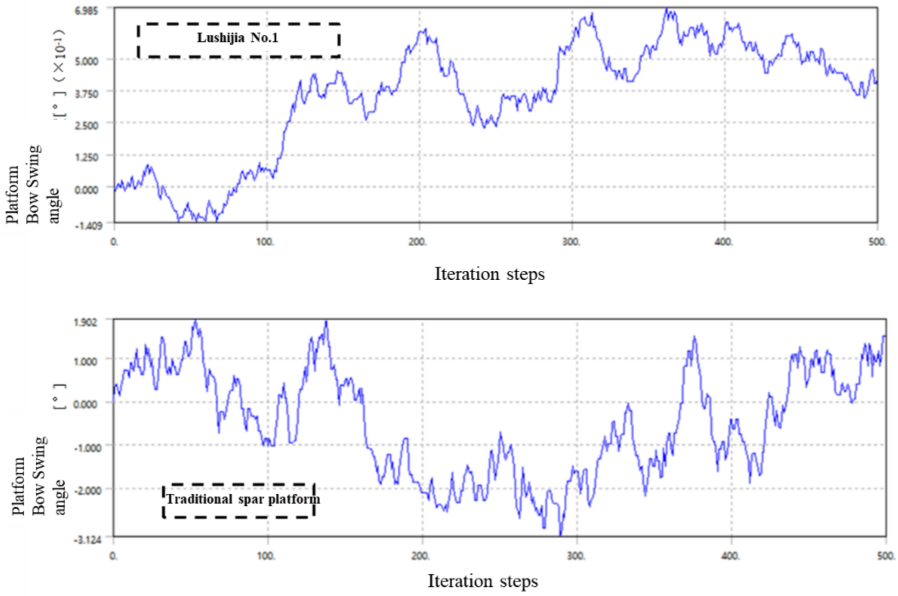

Figure 4. Random response image of the platform under JONSWAP spectrum (bow shake)

From the figure, we can see that the amplitude of change under wave disturbance is significantly smaller for the team-designed "Rustica-1" platform than for the conventional column platform. Both platforms show a large response under the initial disturbance, but with the increase of iteration steps, the response amplitude of both platforms becomes significantly smaller. Compared with the traditional column platform, the amplitude range of the "Lushia No. 1" platform is significantly smaller, and its longitudinal sway angle is roughly concentrated in $0.1° \sim 0.2°$, while the longitudinal sway angle of the traditional column platform is roughly concentrated in $-0.5° \sim 1.5°$, which indicates that the optimized platform is able to resist tilting after wave impact. The ability of the optimized platform to resist tilting after wave impact has been greatly improved.

In terms of bow rocking, the final response of both platforms did not stabilize, and the response amplitude range of the "Lushia 1" platform was concentrated in the range of $-0.15° \sim 0.7°$, while the amplitude range of the traditional column platform was concentrated in the range of $-3° \sim 2°$. Since the wind turbine needs to adjust the yaw angle to receive wind energy, and the bow rocking of the platform will affect the adjustment of the yaw angle of the wind turbine, the optimization of the bow rocking is conducive to the wind turbine to receive wind energy better while ensuring the safety of the whole wind turbine platform.

2.1.3 Wave excitation load of the platform under different wave frequencies

The period range of waves is 0.5s~25s, while the period range of common waves is 0.5s~15s, which corresponds to a frequency range of about 0.4rad/s~1.3rad/s. Therefore, in the research process, it is necessary to pay attention to the frequency of waves to meet the objective range.

The relationship between the wave excitation load (first-order wave force) and the variation of the amplitude response operator with wave frequency for both platforms is studied in the following, and the wave excitation load, which has been introduced in Chapter 4, is essentially a solution of the first-order differential equation MCK (Figures 5 and 6).

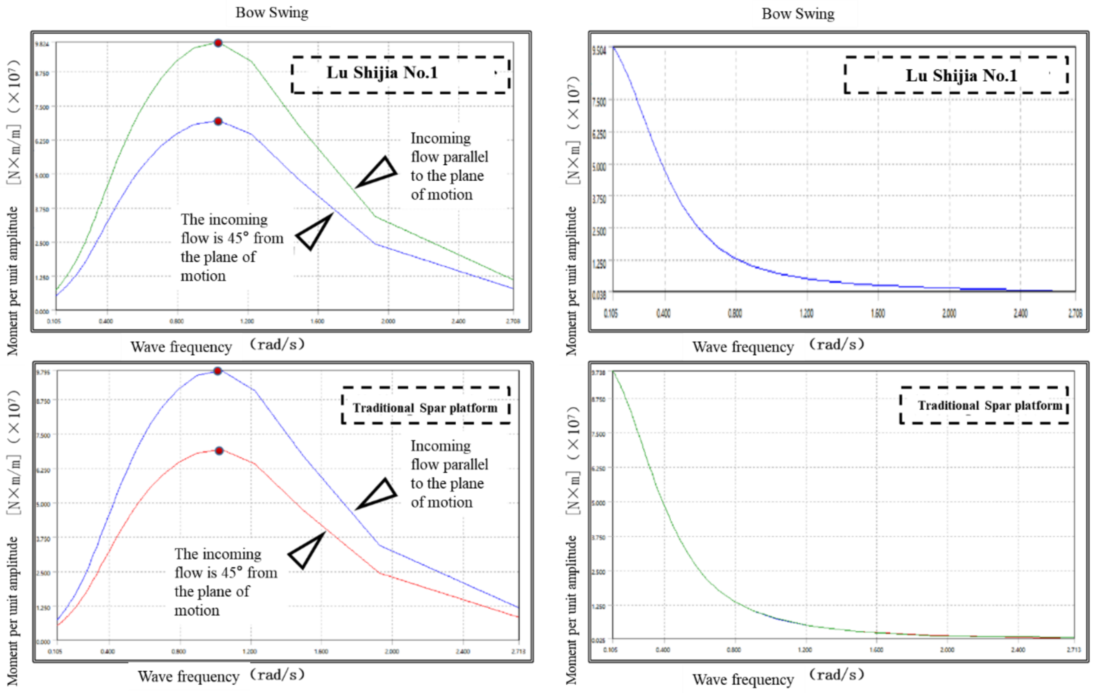

Figure 5. Longitudinal and bow rocking of the platform at wave frequency.

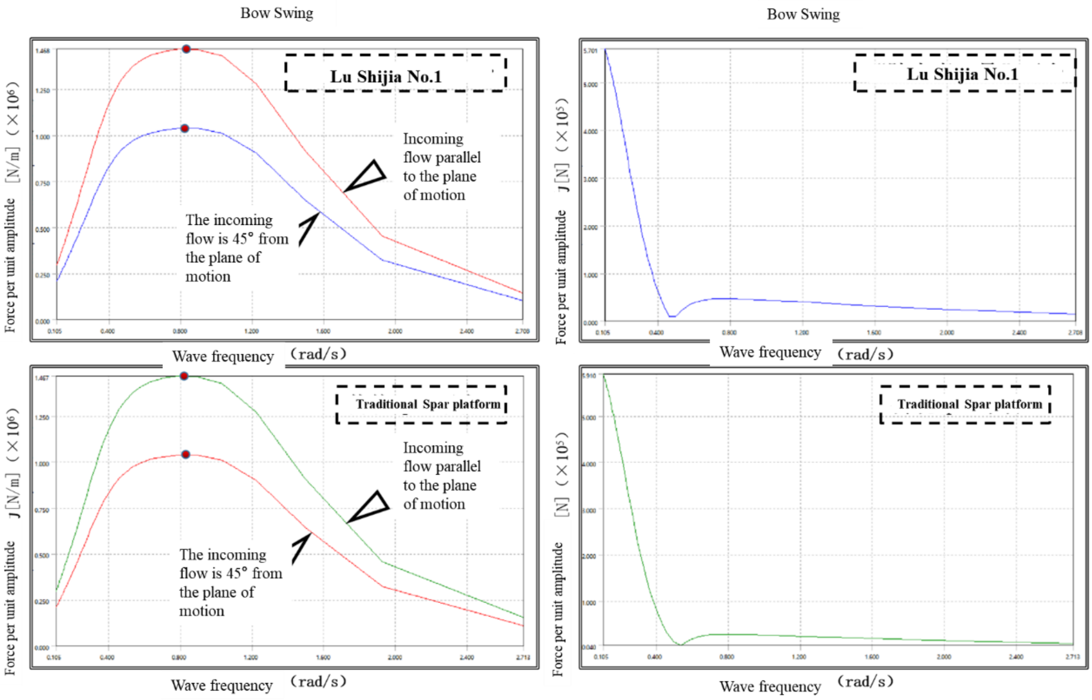

Figure 6. Longitudinal and vertical oscillations of the platform at wave frequency

In order to investigate whether different wave incidence angles have an effect on the shape of wave excitation load images, we set the incidence direction parallel to the direction of motion and the angle of 45°. Different incidence directions have an effect on the peaks of longitudinal rocking and longitudinal oscillation, but almost no effect on the wave frequencies corresponding to the peaks; meanwhile, since bow rocking and drooping oscillation are the corresponding changes of the platform about the z-axis, independent of the incidence direction, the images of different incidence The images of bow sway and droop under different incidence directions are highly overlapping. The wave excitation loads of longitudinal sway and longitudinal oscillation of both platforms increase and then decrease with the increase of wave frequency, where the wave frequency corresponding to the peak of longitudinal sway is around 1.1 rad/s and the wave frequency corresponding to the peak of longitudinal oscillation is around 0.8 rad/s. The design of "Lushia No. 1" is not significantly optimized in reducing the wave excitation loads of longitudinal sway and longitudinal oscillation compared with the traditional column-type platform. Therefore, the difference between the peak values of the two images is not significant.

In terms of bow sway and vertical sway, the wave excitation load is significantly lower than that of the conventional column platform when the wave frequency is small, and the vertical sway wave excitation load has a valley at 0.5 rad/s; both tend to stabilize when the wave frequency increases. In fact, due to the three-float auxiliary platform of the "Lushia 1" platform, the wave excitation load is slightly higher than that of the conventional column platform at stabilization.

2.1.4 Amplitude response operator of the platform at different wave frequencies

The dependent variable RAO amplitude response operator used for the analysis is an engineering statistical concept that can be used to calculate the behavior of the platform when operating in the sea. It corresponds to the amplitude of the motion of a certain degree of freedom caused by a regular wave flowing through the platform at each frequency and amplitude of 1(Figure 7).

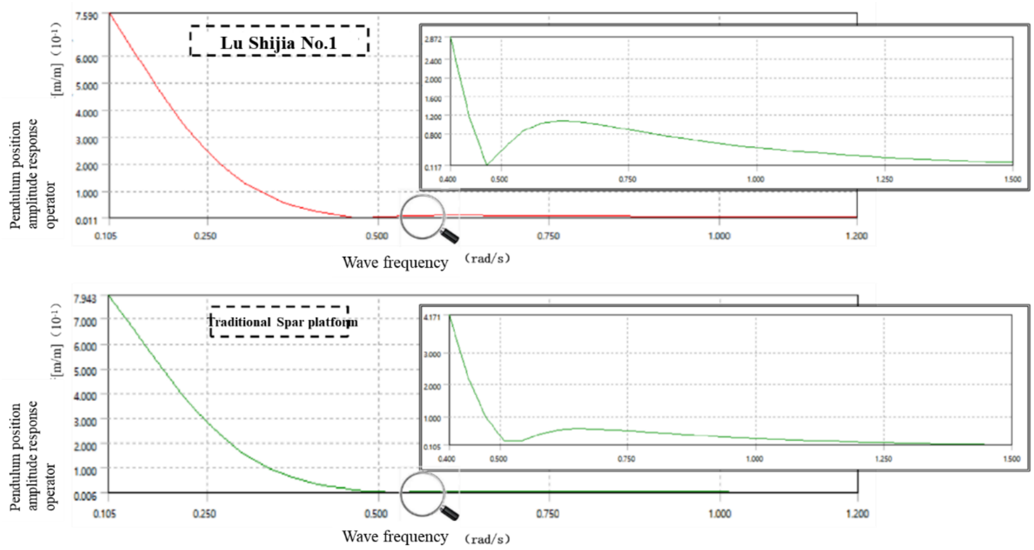

Figure 7. pendulous RAO of the platform under wave frequency

Since the frequency range of common waves is about 0.4rad/s~1.3rad/s, the droop images are scaled up in this interval. The optimized platform responds better than the conventional platform at low wave frequencies, and the RAO valley value corresponds to a lower wave frequency, which corresponds to a wave frequency of about 0.47 rad/s; while the situation at higher wave frequencies is similar to the wave excitation load image - the RAO of the conventional column platform is slightly smaller than that of the "Lucega 1"(Figure 8).

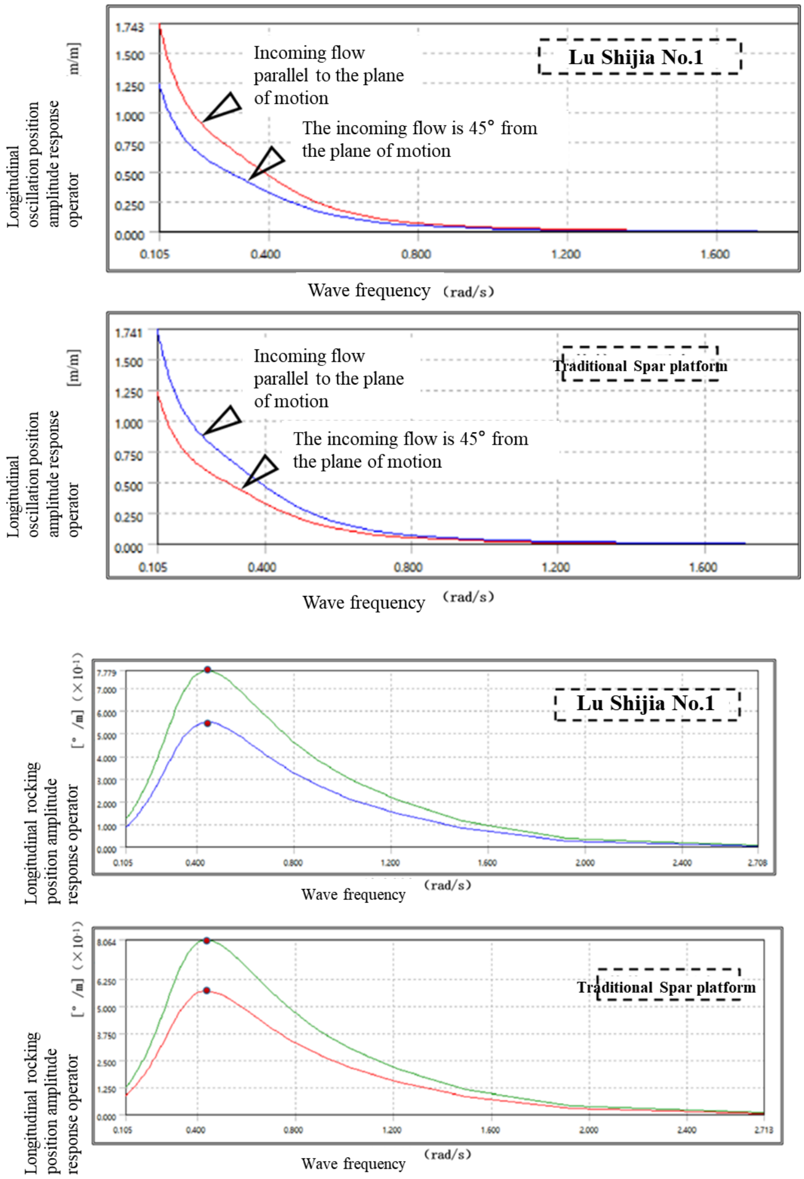

Figure 8. longitudinal oscillation and longitudinal rocking RAO of the platform at wave frequency

In the aspect of longitudinal oscillation and longitudinal shaking, the incident wave is also set in two directions, and through comparative analysis, it is concluded that the optimized platform in longitudinal oscillation has no obvious change compared with the traditional column platform, while the optimized platform in longitudinal shaking has significant changes, and the wave frequency corresponding to its peak has not changed significantly but its peak has been significantly reduced, and the longitudinal shaking performance has been optimized to ensure the safety of the platform.

2.2. Time domain full coupling analysis of the platform motion response

FAST is used to simulate the time domain motion response of the platform. In the calculation of the offshore floating wind turbine, FAST cannot perform 3D radiation and winding calculation, so it needs to rely on the hydrodynamic data of $ANSYS\quad AQWA$ as the input file. In each calculation step, FAST calculates the load on the floating foundation according to its position and iterates on this basis to obtain the position of the floating foundation in the next time step until the end of the calculation, while the software focuses on the relationship between the power generation-related parameters of the platform and time, which cannot be done by AQWA.

The two comparison platforms are the semi-submersible platform and the Ruzika-1. In terms of hydrodynamics, the JONSWAP wave spectrum is still used as the random wave spectrum, while the water depth, wave height, wave number, waveform and other parameters are controlled consistently, and the wave level is set to medium (the effective wave height is set to 4m); in terms of wind turbine control, the H_∞ controller mentioned above is used to adjust the collective pitch angle of the blades, and the power generation of the generator at the initial moment is set to 0. The initial parameters of each part of the wind turbine are set to 0 except $\omega_r = 12.1rpm$.

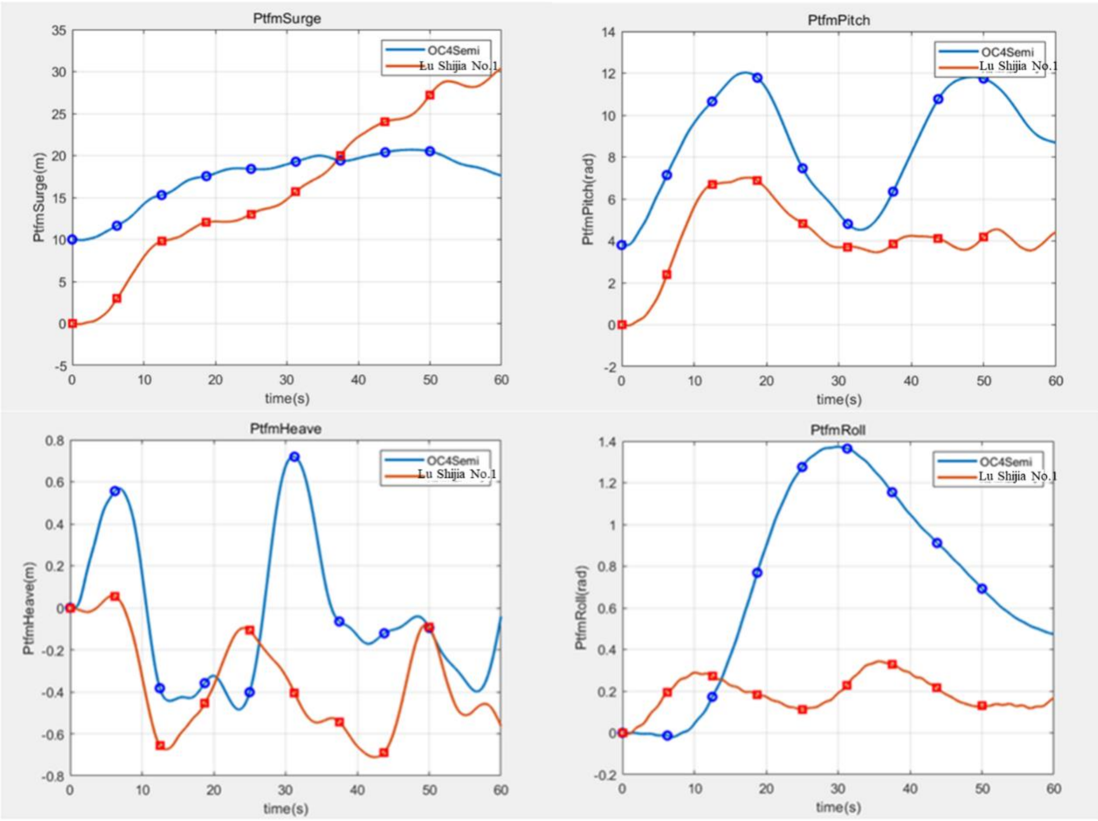

Figure 9. FAST simulation results - motion response under low-level waves

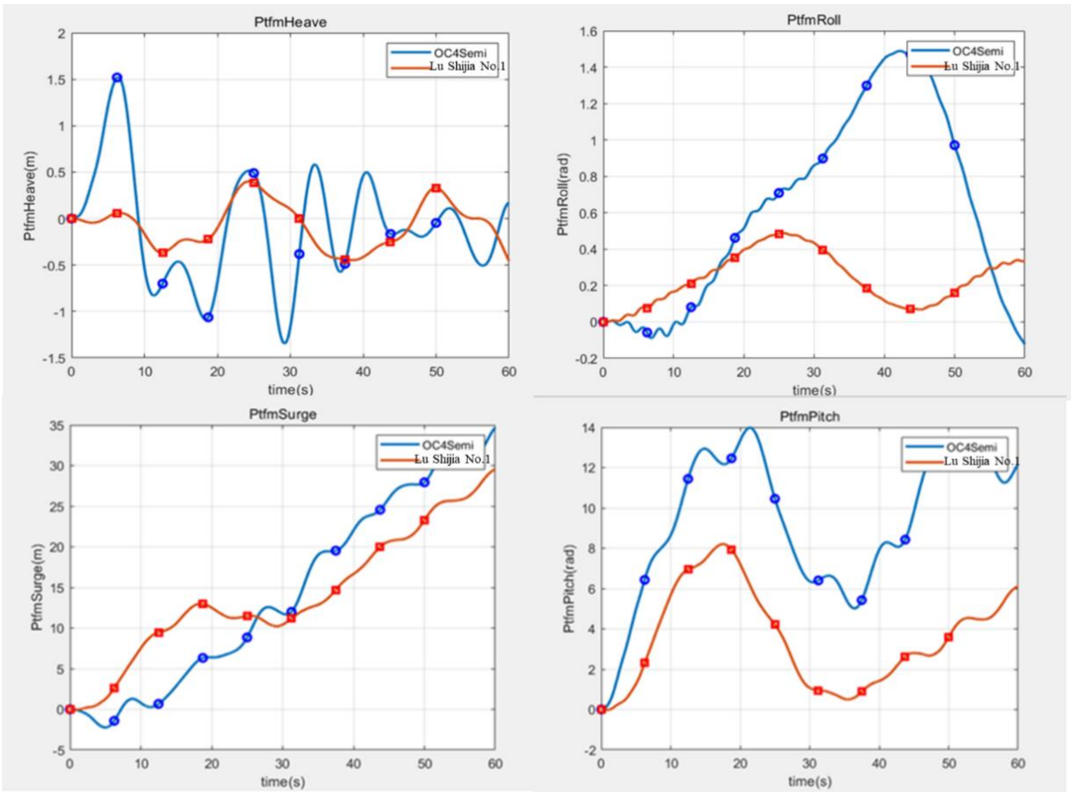

Figure 10. FAST simulation results - motion response under moderate waves

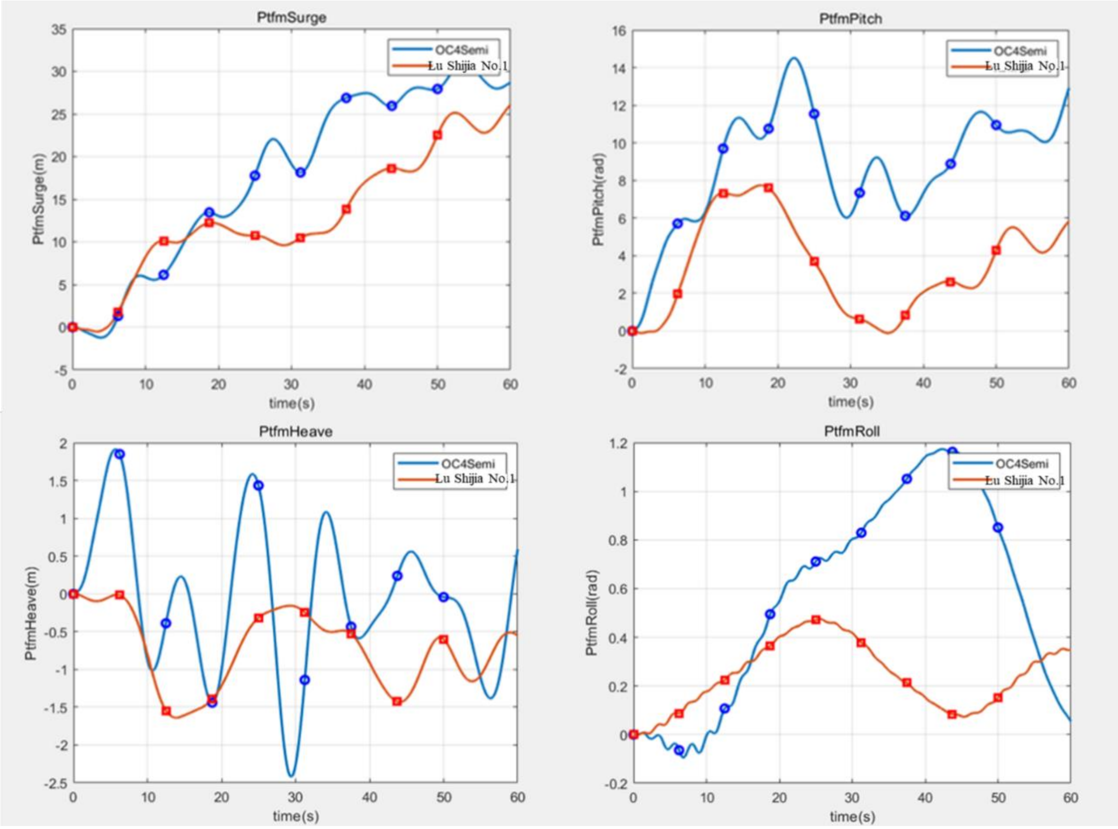

Figure 11. FAST simulation results - motion response under advanced waves

The above time-domain simulation of the motion response of the platform was carried out in the background of three sea states (Figures 9, 10, 11). It can be seen that under the three sea conditions, the pendulum performance of the "Ruzga-1" platform is greatly improved compared with the semi-submersible OC_4 platform by using the column support platform as the main body, and the amplitude of pendulum Heave is reduced by more than half. At the same time, except for the longitudinal rocking Surge, all other types of motion modes are improved compared with the semi-submersible platform.

In terms of the power generation of the platform turbine (Figure 12), we found that the power generation and the angular velocity of the impeller and rotor of the two turbines were highly overlapping at the beginning of the time, but as time went on, the power generation of the Ruzika-1 was significantly more stable than that of the semi-submersible platform, the key of which is the same The key to this is the generally higher blade speed under the same conditions - which has less impact on the power generation because the motion modes of the platform vary less over time. Under different sea states, the amplitude of the platform motion has little effect on the generator power, so there is no significant change in the image trends of the two platforms in terms of wind turbine power generation parameters under different sea state simulations.

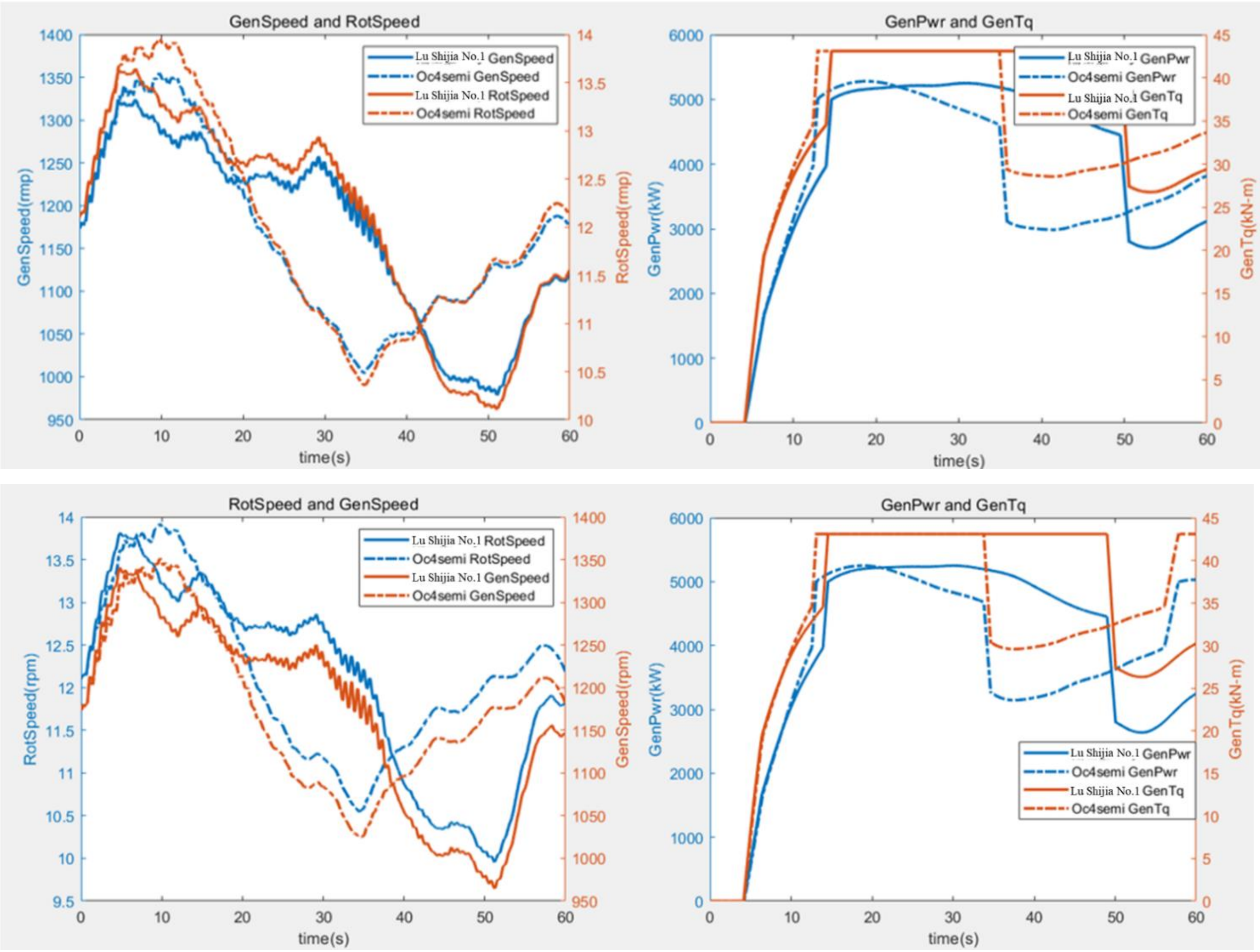

Figure 12. FAST simulation results - variation of wind turbine power generation parameters

3. Conclusions

In order to improve the response of the platform under the waves, a self-locking sliding sleeve system is installed on the platform with a shaft guide, and three wave energy generating floats are connected to the sleeve in three directions by means of spars to complete Combined power generation. A complete set of computational theory of platform force and motion response analysis is constructed for the designed new wind turbine platform, and the H_{∞} controller of wind turbine regulation is optimized. In the simulation fitting, the model of "Lushia I" built by Solidworks is imported into A$ANSYA\quad AQWA$ to calculate and analyze its frequency domain hydrodynamic performance, and its time domain response process is analyzed by FAST and compared with the traditional floating platform.

References

[1] Shah, K. A., Meng, F., Li, Y., Nagamune, R., Zhou, Y., Ren, Z., \& Jiang, Z. (2021). A synthesis of feasible control methods for floating offshore wind turbine system dynamics. Renewable and Sustainable Energy Reviews, 151. doi: 10.1016/j.rser.2021.111525

[2] Homer, J. R., \& Nagamune, R. (2018). Physics-Based 3-D Control-Oriented Modeling of Floating Wind Turbines. IEEE Transactions on Control Systems Technology, 26(1), 14-26. doi:10.1109/tcst.2017.2654420

[3] Muliawan, M. J., Karimirad, M., \& Moan, T. (2013). Dynamic response and power performance of a combined Spar-type floating wind turbine and coaxial floating wave energy converter. Renewable Energy, 50, 47-57. doi: 10.1016/j.renene.2012.05.025 %

[4] Muliawan, MJ, Karimirad, M, Moan, T, \& Gao, Z. "STC (Spar-Torus Combination): A Combined Spar-Type Floating Wind Turbine and Large Point Absorber Floating Wave Energy Converter — Promising and Challenging." Proceedings of the ASME 2012 31st International Conference on Ocean, Offshore and Arctic Engineering. Volume 7: Ocean Space Utilization; Ocean Renewable Energy. Rio de Janeiro, Brazil. July 1–6, 2012. pp. 667-676. ASME. https://doi.org/10.1115/OMAE2012-84272

[5] Ahn, H.-J., \& Shin, H. (2019). Model test and numerical simulation of OC3 spar type floating offshore wind turbine. International Journal of Naval Architecture and Ocean Engineering, 11(1), 1-10. doi: 10.1016/j.ijnaoe.2017.09.010

[6] Cortes Sanchez, C. J. (2018). Wind and wave disturbance rejection control of floating offshore wind turbines (T). University of British Columbia. Retrieved from https://open.library.ubc.ca/collections/ubctheses/24/items/1.0365588.

[7] A Taher, M Farshadnia, M R Mozdianfard. Optimal gain scheduling controller design of a pitch-controlled VS-WECS using DE optimization algorithm [J]. Applied Soft Computing Journal, 2013, 13(5): 2215-2223.

[8] Zhao Shuchen, Numerical analysis of a new Spar floating fan with full coupling of aerodynamic-hydrodynamic-mooring [D], 2021, Dalian University of Technology. Page 86.

[9] Hu T. M., Design study of a floating wind and wave energy hybrid utilization system [D], 2020, Jiangsu University of Science and Technology. Page 108.

[10] Wang D., Numerical study on the hydrodynamic performance of oscillating float type wave energy generation device [D], 2019, Shanghai Jiao Tong University. Page 84.